Electron Beam Lithography Simulation for Mask Making, Part VI: Comparison of 10 and 50 kV GHOST Proximity Effect Correction

Chris A. Mack
KLA-Tencor, 8834 N. Capital of Texas Hwy, Suite 301, Austin Texas 78759
E-mail: chris_mack@finle.com

Abstract

GHOST uses two exposures, the primary dose and its complement, in an attempt to equalize the effects of backscattering and reduce proximity effects. Unfortunately, image contrast is reduced compared to exposures done without GHOST. A simplified raster scan theory is developed in order to examine the effects of backscattering and GHOST proximity correction on the quality of the images produced. Electron beam lithography simulation is used to examine the effect of spot size and voltage on the spot image generated in 400 nm of ZEP 7000 resist, and the effects of GHOST on proximity effects and process latitude.

Keywords: ProBEAM/3D, e-beam lithography modeling, GHOST, proximity effect correction.

1. Introduction

The necessity for performing proximity correction on electron beam mask lithography will increase as the device generation migrates from 180 to 130 nm. GHOST proximity effect correction is one proposed method to improve CD linearity and to reduce backscatter-induced proximity effects. Along with migration to smaller feature sizes, increasing the accelerating voltage has major benefits in reducing the forward scatter of the incident beam. GHOST uses two exposures, the primary dose and its complement, in an attempt to equalize the effects of backscattering and reduce proximity effects. Because of the way the aerial image for GHOST correction is built, image contrast will be less favorable than exposures done without GHOST. At 50 keV, however, improved forward scatter (and the smaller spot sizes that this enables) means that GHOST has much less of an impact on process latitude than at 10 keV. In this paper, simulation of the electron beam imaging process using ProBEAM/3D examines the effect of spot size and voltage on the spot image generated in 400 nm of ZEP 7000 resist. Results show the benefits of using the higher voltage. This paper also uses simulation to examine the effects of GHOST proximity correction for both 10 and 50 keV imaging, and the impact of proximity correction on process latitude.

2. Theory of Raster Scan Imaging

Raster scan imaging can be thought of as the formation of an image by the summation of many spatially distinct basis images of (possibly) differing energies [1,2]. In practice, this summation is always “incoherent”, meaning the energy deposited into the resist material for each basis image is added together to form the total energy of the total image. A basis image, for example, could be simply the intensity of the spot of a laser beam as it is projected onto the surface of a substrate (or more correctly, deposited into a photoresist film). For the simplest raster scan imaging scheme, only one basis image is used, a so-called *spot* or *pixel* image, and each basis image has equal energy. Ignoring, for the purposes of this discussion, the distribution of energy through the thickness of the resist film, the raster scan image $I(x,y)$ can be described as the summation of many spatially-shifted basis images.

$$I(x,y) = \sum_{i=1}^{N} P(x - x_i, y - y_i) \qquad (1)$$

where $P(x,y)$ is the image of a single pixel or spot, and the set of points (x_i,y_i) represent the centers of each pixel that are being summed to form the final image (i.e., the address grid).

For both laser beam and electron beam raster scan writing tools, the pixel image can be fairly approximated as a Gaussian beam. As a simple starting place, let us assume that the only basis image being used is a symmetric Gaussian pixel. Normalizing the pixel to have a peak intensity of 1,

$$P(x,y) = \exp\left(-\frac{x^2+y^2}{2\sigma^2}\right) = \exp\left(-\frac{x^2}{2\sigma^2}\right)\exp\left(-\frac{y^2}{2\sigma^2}\right) \qquad (2)$$

where the width of the Gaussian is defined by σ. Assume that the raster scan strategy being employed uses a fixed address grid with grid spacings Δx and Δy. The image being produced is then given by equation (1) with address grid points turned either on or off.

2.1. Image of a Single Spot

Two very simple examples will illustrate the formation of a raster scan image. First, consider the simplest image – a single spot. In this case, only one address grid point is "on" so that the total image is just

$$I_{spot}(x,y) = \exp\left(-\frac{x^2+y^2}{2\sigma^2}\right) \qquad (3)$$

Note that this is also the general result of the image in the vicinity of $x = y = 0$ whenever Δx and Δy are much greater than σ.

Using this simple result, we can derive some of the basic lithographic properties of the image. First, where is the "edge" of the image? In other words, when this image is printed in resist, where will the edges of the resist lie? Although this is a rather complicated question, it can be simplified by assuming the response of the resist to a Gaussian-shaped image is such that the resist edge will occur at an normalized energy threshold of I_{th}. For example, picking $I_{th} = 0.5$ would produces edges corresponding to the full width half maximum (FWHM) point of the image. In optical lithography, it has been shown empirically that most resists have near optimum performance when $I_{th} \approx 0.3$. For an arbitrary threshold intensity, the position of the left edge (at $y = 0$) is given by

$$x_{edge} = -\sigma\sqrt{2\ln(1/I_{th})} \qquad (4)$$

where the center of the spot is at $x = 0$. As an example, the FWHM ($I_{th} = 0.5$) width ($= 2\,|x_{edge}|$) is equal to 2.355σ.

For the image of a spot, what is the quality of the image? One of the most useful metrics of image quality is the image log-slope: the slope of the logarithm of the image at the nominal photoresist edge. For the Gaussian spot image, the image log-slope is just

$$log - slope \;=\; \left.\frac{d\ln I}{dx}\right|_{x_{edge}} \;=\; \frac{\sqrt{2\ln(1/I_{th})}}{s} \qquad (5)$$

It is quite apparent that equation (5) predicts improved image quality (improved log-slope) for a smaller spot beam (i.e., smaller σ). The image log-slope can be normalized by multiplying by the desired feature width to give the dimensionless normalized image log-slope (NILS). For this case, the NILS becomes

$$NILS \;=\; 4\ln(1/I_{th}) \qquad (6)$$

If I_{th} = 0.5 the NILS will have a value of about 2.8. For I_{th} = 0.3 the NILS will become about 4.8. This increasing NILS with lower threshold intensity means that resist images printed at these lower threshold intensities will have much greater linewidth control.

2.2. Image of an Edge

A second, somewhat less trivial, example is the image of an edge where all pixels such that $x_i \geq 0$ are turned on.

$$I_{edge}(x,y) \;=\; A(y)\sum_{n=0}^{\infty}\exp\left(-\frac{(x-n\Delta x)^2}{2s^{\,2}}\right) \qquad (7)$$

where *A(y)* is the result of summing all pixels in the y-direction. An interesting special case occurs when the address grid becomes infinitely small. For such a case, the summation in equation (7) becomes an integral, *A(y)* becomes a constant (= $\sqrt{2p\,s}$), and an "ideal edge" image can be formed:

$$I_{ideal-edge}(x,y) \;=\; \frac{1}{2}\,\mathrm{erfc}\left(-\frac{x}{\sqrt{2}\,s}\right) \qquad (8)$$

where the image has been normalized to have a peak value of 1 and erfc(z) is the complimentary error function. Note that this image is "ideal" only in the sense that it is a limiting behavior and, in fact, may not be the best image for a particular application.

Where is the edge for this image of an edge? For two cases, Δx » σ and Δx « σ, the result can be determined analytically. When the address grid is much bigger than the Gaussian spot size, the edge position is just given by equation (4) since the edge is influenced almost exclusively by the nearest spot. When the address grid is much smaller than the spot size, a simple result is also possible. Consider first the limiting case of an infinitely small address grid. Picking a specific threshold intensity, equation (8) can be solved for the position of the edge.

$$\begin{aligned} For\ I_{th} &= 0.3, \quad x_{edge} \;\approx\; -0.523\,s \\ For\ I_{th} &= 0.5, \quad x_{edge} \;=\; 0 \end{aligned} \qquad (9)$$

When the address grid size Δ*x* is bigger than zero, but still much smaller than the spot size, the edge position becomes

$$For\ I_{th} = 0.3, \quad x_{edge} \approx -0.523\sigma - \Delta x/2$$
$$For\ I_{th} = 0.5, \quad x_{edge} = -\Delta x/2 \qquad (10)$$

The image quality of the raster scan printed edge can again be described by the image log-slope. Defining the log-slope at the edge position given by equation (10), the two cases are again $\Delta x \gg \sigma$ and $\Delta x \ll \sigma$. If the address grid is much larger than the spot size, the image log-slope is given by equation (5), the log-slope of a single spot. When the address grid is much smaller than the spot size, equation (8) can be used to derive the log-slope.

$$For\ I_{th} = 0.3, \quad log-slope \approx \frac{1.16}{\sigma}$$
$$For\ I_{th} = 0.5, \quad log-slope = \frac{\sqrt{2/\pi}}{\sigma} \approx \frac{0.798}{\sigma} \qquad (11)$$

As in the case of a single spot, both a smaller spot size and a lower I_{th} results in a better quality image of the edge. Note that a desire to improve image quality by using a lower I_{th} will necessitate the use of a "bias", a difference between the actual resist edge position and the nominal position half way between the rows of on and off pixels.

2.3. Effects of E-Beam Backscattering

The above discussion of the nature of raster scan imaging assumed a simple Gaussian basis function. For electron beam writing, scattering within the resist and the substrate can lead to an energy distribution in the resist that is more complicated than a simple Gaussian. Many authors have noted that this backscattering of electrons leads to a distribution that can be reasonably approximated by a double Gaussian. In one dimension, this could take the form

$$P(x,y) = (1-\beta)\exp\left(-\frac{x^2+y^2}{2\sigma^2}\right) + \beta\exp\left(-\frac{x^2+y^2}{2\sigma_B^2}\right) \qquad (12)$$

where σ_B defines the width of the backscatter component of the distribution ($\sigma_B > \sigma$) and β describes its strength (roughly equivalent to the fraction of electrons that are backscattered per unit area).

Consider an edge made of the summation of these double Gaussian spots. For the ideal edge case (infinitely small address grid), the edge becomes the sum of two complimentary error functions:

$$I_{ideal-edge}(x) = \frac{1}{2}\left[(1-\beta')\text{erfc}\left(-\frac{x}{\sqrt{2}\sigma}\right) + \beta'\text{erfc}\left(-\frac{x}{\sqrt{2}\sigma_B}\right)\right] \qquad (13)$$

where $$\beta' = \frac{\beta\sigma_B^2}{(1-\beta)\sigma^2 + \beta\sigma_B^2}$$

The impact of this scattering on the log-slope of the image at the edge is given by

$$For\ I_{th} = 0.5, \quad log - slope \ = \ \sqrt{\frac{2}{\pi}}\left(\frac{1-\beta'}{\sigma} + \frac{\beta'}{\sigma_B}\right) \tag{14}$$

It is clear from this equation that both larger β' and larger σ_B result in a lower log-slope. As an example, 10 keV exposure of 400nm thick resist on a mask blank with a 250nm size spot (FWHM) would typically produce $\sigma \approx$ 115nm, $\sigma_B \approx$ 510nm, and $\beta \approx 0.055$. This would give a $\beta' \approx 0.53$. The log-slope in this case is about 40% lower than if there had been no scattering. For a 50 keV exposure using a 100nm spot size (FWHM), $\sigma \approx$ 43nm, $\sigma_B \approx$ 6.5µm, and $\beta \approx 0.000044$. This would result in a value of $\beta' \approx 0.50$ (curiously similar to the value obtained for 10 keV). The log-slope of the image of an isolated edge at 50 keV is reduced by 50% due to backscattering. While the percent reduction in log-slope due to backscattering is larger at 50 keV than at 10 keV, the smaller spot sized used at 50 keV more than makes up for this difference.

2.4. The Effects of Ghost Exposure

Ghost exposure is a means to correct for the varying affects of backscattering as a function of pattern density. This is accomplished by subjecting the resist to a second exposure (after the normal writing of the pattern) comprised of a negative of the original pattern, exposed using a large spot and with a dose smaller than the original. In other words, the goal of the ghost exposure is to mimic the backscattered portion of the exposure in the nominally unexposed areas, thus equaling out the impact of this unwanted effect. For example, the ghost correction pattern for the isolated edge of equation (13) would be an opposite-facing edge with lower energy:

$$I_{ghost-edge}(x) \ = \ \frac{\alpha}{2}\left[(1-\beta'_g)\mathrm{erfc}\left(+\frac{x}{\sqrt{2}\sigma_g}\right) + \beta'_g\,\mathrm{erfc}\left(+\frac{x}{\sqrt{2}\sigma_B}\right)\right] \tag{15}$$

where σ_g is the width of the ghost exposure spot and α is the ghost dose relative to the normal exposure dose. If the ghost spot width is adjusted to equal the backscatter Gaussian width (i.e., $\sigma_g = \sigma_B$), the ghost edge simplifies to

$$I_{ghost-edge}(x) \ = \ \frac{\alpha}{2}\mathrm{erfc}\left(+\frac{x}{\sqrt{2}\sigma_B}\right) \tag{16}$$

Adding the ghost pattern to the original exposure of equation (13),

$$I_{total-edge}(x) \ = \ \frac{1}{2}\left[(1-\beta')\mathrm{erfc}\left(-\frac{x}{\sqrt{2}\sigma}\right) + \beta'\mathrm{erfc}\left(-\frac{x}{\sqrt{2}\sigma_B}\right)\right] + \frac{\alpha}{2}\mathrm{erfc}\left(+\frac{x}{\sqrt{2}\sigma_B}\right) \tag{17}$$

By letting $\alpha = \beta'$, an interesting result occurs: the backscattered pattern becomes a simple, uniform background dose.

$$I_{total-edge}(x) \ = \ \frac{1}{2}\left[(1-\beta')\mathrm{erfc}\left(-\frac{x}{\sqrt{2}\sigma}\right)\right] + \beta' \tag{18}$$

The impact of this optimized ghost pattern on the log-slope of the edge can now be determined.

$$For\ x_{edge} = 0, \quad log - slope \ = \sqrt{\frac{2}{p}}\left(\frac{1-b'}{1+b'}\right)\left(\frac{1}{s}\right) \qquad (19)$$

Thus, ghosting reduces the log-slope even further. For the cases described previously (where $\beta' \approx 0.5$ for both 10 keV and 50 keV), the log-slope is decreased by 35 - 45% compared to the no-ghost case. Figure 1 shows how the ghost proximity correction scheme affects this image of an edge for the 10 keV case.

Interestingly, since β' is about the same for both 10 keV and 50 keV, the use of an optimum GHOST exposure condition has the same relative impact on the log-slope of an isolated edge compared to the ideal case of no backscattering. The only advantage that the 50 keV exposure gives is the smaller spot size (the smaller value of σ in equation (19)) that in turn produces a higher image log-slope. Since, in general, one can expect the minimum forward scattered spot size in resist (σ) to be at least twice as large at 10 keV than at 50 keV, the image log-slope of an isolated edge with an optimum GHOST exposure should be at least twice as high at 50 keV than at 10 keV.

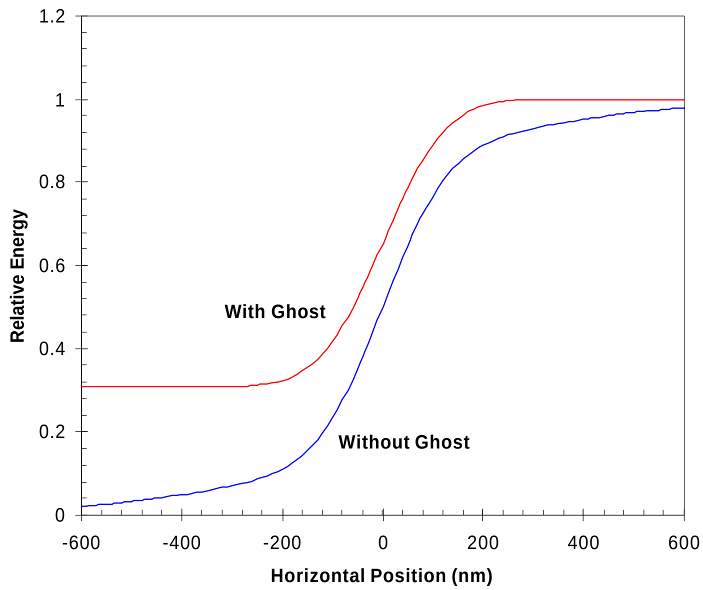

Figure 1. The impact of an optimized ghost exposure on an ideal edge (with σ = 100m, σ_B = 400nm, and β = 0.1).

3. Simulation Results

ProBEAM/3D v6.2 was used to simulate typical raster scan imaging situations at 10and 50 keV, with and without GHOST. Parameters for ZEP 7000 (with ZED 750 developer), measured previously for 10 keV exposure [1], were assumed to be remain the same at 50 keV. Obviously this assumption should be confirmed experimentally, but it suits the purposes here to compare voltages using an identical resist. 400nm of resist on 100nm of chrome on glass was used. Figure 2 shows the results of the Monte Carlo scattering calculations, providing the average energy deposited in resist per electron. The difference between forward and back scattering energies for the two voltages is apparent. In Figure 3, these scattering results are convolved with a Gaussian beam shape to predict the deposited energy for a single spot exposure. Again it is obvious that the 50 keV exposure produces less forward scattering (and thus more vertical energy contours near the edge of the spot) compared to the 10 keV case. It is also obvious that the 50 keV exhibits a much longer backscatter range.

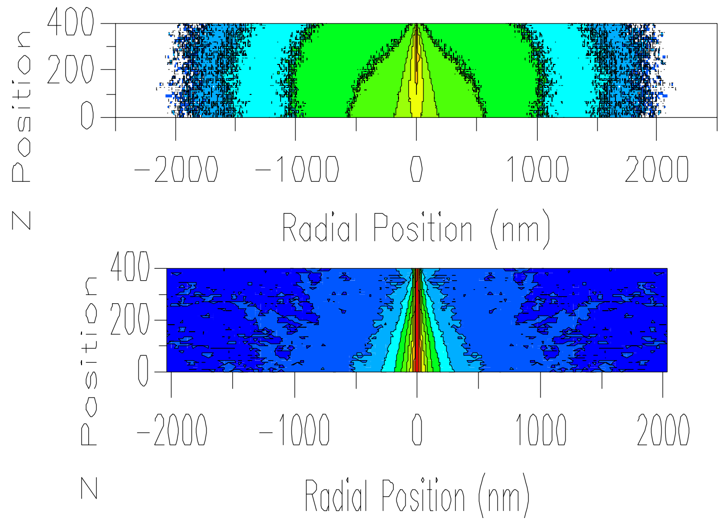

Figure 2. Monte Carlo simulations of electron energy distributions (contours of log-energy per electron). Top graph show results for 10 keV electrons, bottom for 50 keV.

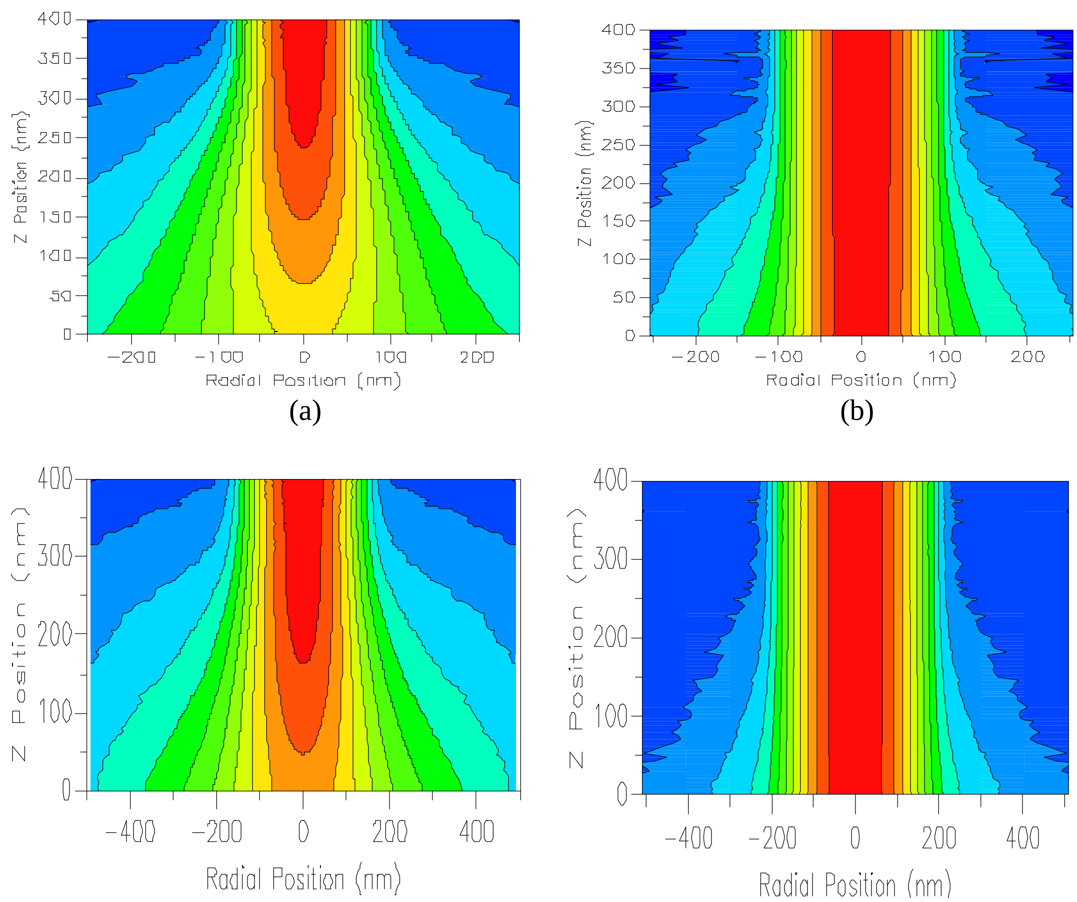

Figure 3. Energy distributions in resist for a single spot exposure for (a) 10 keV, 60 nm FWHM spot size, (b) 50 keV, 60 nm spot size, (c) 10 keV, 120 nm spot size, and (d) 50 keV, 120 nm spot size.

The above simulations show clearly the impact of forward scattering on the lithographic results. It is not as clear what the impact of the different backscattering behaviors between these two voltages will be. To see this effect, one must look for proximity effects. One simple proximity effect measure is to examine how the printed resist linewidth of a line/space pair varies with changing spacewidth.

Figure 4 shows the proximity effect for 10 keV exposure of an 800 nm line. The dose was adjusted to give the correct linewidth for the equal line/space case. As can be seen, when no proximity correction is used, the isolated line (represented by the large pitches of the figure) shows a 60 nm bias due to the increased backscatter of the larger spaces. By applying a GHOST correction with a 1000 nm spot size at a dose of 40% of the primary dose, nearly perfect printing through pitch is obtained. Obviously, GHOST is quite effect at reducing this type of proximity effect to within acceptable levels. As mentioned earlier, however, the price to be paid is the loss of linewidth control due to the reduced log-slope of the exposure gradient at the resist edge. Figure 5 shows how develop latitude is reduced through the use of GHOST as 10 keV.

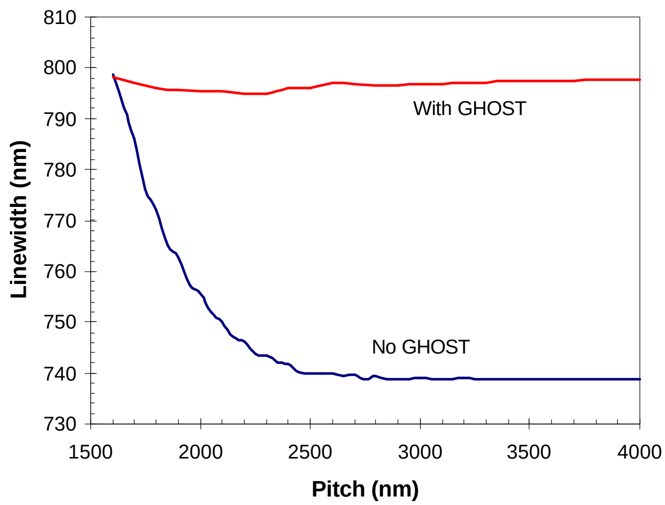

Figure 4. Simulation of 10 keV proximity effects shown by printing an 800 nm line with varying pitch with and without GHOST. The primary exposure used a 250 nm spot on a 50 nm grid. For the GHOST case, the GHOST exposure used a 1000 nm spot at a dose of 40% of the primary dose.

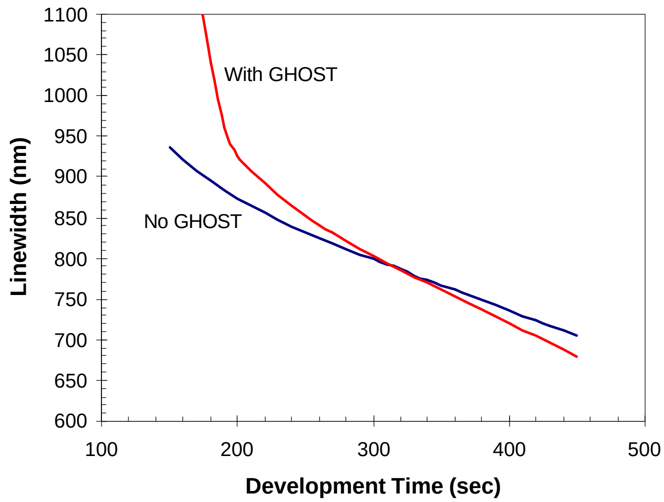

Figure 5. Impact of GHOST on process latitude is shown at 10 keV as linewidth as a function of development time using the same conditions as Figure 5.

As Figure 6 shows, proximity effects at 50 keV are much worse than at 10 keV. GHOST is also effective at reducing proximity effects at 50 keV. It is apparent that the GHOST parameters chosen for this simulation are not optimum, and no attempt was made to find the optimum parameters for this system. It appears that higher GHOST doses are required, however.

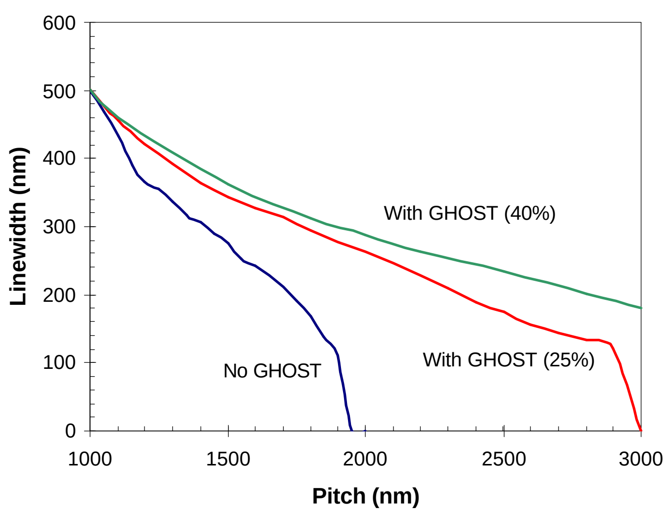

Figure 6. Simulation of 50 keV proximity effects shown by printing an 500 nm line with varying pitch with and without GHOST. The primary exposure used a 100 nm spot on a 25 nm grid. For the GHOST case, the GHOST exposures used a 6000 nm spot at doses of 25% and 40% of the primary dose.

4. Conclusions

Through the use of a simple aerial image theory of raster scan imaging and through full electron beam lithography simulations, the use of GHOST proximity effect correction for 10 keV and 50 keV exposure was presented. Simulation showed what is commonly know in the industry: higher accelerating voltages will reduce forward scattering, but at the cost of a longer range of backscattering. As the aerial image theory predicts, reduced forward scattering resulting in a higher energy gradient near the line edge, which in turn will provide increased linewidth control in the presence of processing and exposure errors. GHOST, while reducing proximity effects, has the detrimental side effect of reducing this energy gradient. For 10 keV, GHOST is very effective at eliminating the through pitch type of proximity effect. However, the already shallow energy gradient produced by the forward scattering at this voltage means that the final ghosted image will have an exceedingly low energy gradient.

At 50 keV, the improved forward scattering results in a significantly better energy gradient at the feature edge. It was not clear at the beginning of this study, however, how much GHOST would impact this fundamentally better behavior. Simple theory predicted the need for a GHOST dose at about 50% of the primary exposure, the same as for 10 keV. However, while a smaller than expected GHOST dose proved adequate at 10keV, the same 40% GHOST dose seemed too small at 50 keV. While no attempt was made to find the optimum dose, it seems apparent that a higher dose is required. These higher doses will in turn further reduce the image log-slope of the total dose. Fortunately, the smaller spot size possible at 50 keV still provides more benefit than is taken away by the GHOST proximity correction.

Although this work shows the effectiveness of GHOST at reducing proximity effects, other proximity correction schemes that don't reduce the image quality in the same way would certainly be desirable. Further, any imaging scheme that can produce a spot (basis function) with a fundamentally higher log-slope than a Gaussian spot will always lead to improved image quality in a raster scan imaging tool.

5. Acknowledgments

The author wishes to thank Chuck Sauer for many useful discussions.

6. References

1. C. Sauer and C. A. Mack, "Electron Beam Lithography Simulation for Mask Making, Part IV: Effect of Resist Contrast on Isofocal Dose," *Photomask and X-Ray Mask Technology VI*, *Proc.*, SPIE Vol. 3748 (1999) pp. 27-40.

2. C. A. Mack and C. Sauer, "Electron Beam Lithography Simulation for Mask Making, Part V: Impact of GHOST proximity effect correction on process window," *19th Annual BACUS Symposium on Photomask Technology and Management*, *Proc.*, SPIE Vol. 3873 (1999) pp. 2-20.